LAWRENCE
LIVERMORE
NATIONAL
LABORATORY

LLNL-PROC-604413

Flat Plate FCG Experimental System for Material Studies

D. A. Goerz, D. B. Reisman, J. B. Javedani, J. T. Paladichuk, D. E. Hare, L. J. Tallerico, G. G. Earley, R. M. Kuklo, A. D. White

November 27, 2012

2012 International Conference on Megagauss Magnetic Field Generation and Related Topics
Maui, HI, United States
October 14, 2012 through October 19, 2012

Disclaimer

Flat Plate FCG Experimental System for Material Studies

D. A. Goerz, D. B. Reisman, J. B. Javedani, J. T. Paladichuk, D. E. Hare, L. J. Tallerico,
G. G. Earley, R. M. Kuklo, and A. D. White,
Lawrence Livermore National Laboratory
Livermore, CA USA
<goerz1@llnl.gov>

Abstract— **Magnetic flux compression generators (FCGs) driven by high explosives can produce extremely high magnetic fields that are useful in accelerating metal liners and sample materials to high velocities to study their properties. For material studies requiring extremely high energy and applied pressures, explosive FCGs can far surpass the typical performance of capacitor based systems. Flat plate generators (FPGs) are useful in many flux compression applications. They are well suited for doing material studies in planar geometries, and they enable the use of certain diagnostic techniques, most notably flash X-ray radiography, which would be difficult if not impossible to utilize in coaxial geometries. Typical flat-plate generators have rather slow-rising output currents. This can cause loads to deform significantly before the highest rate of current gain from the generator can be reached. Shearer et al. at LLNL overcame this handicap by developing a version of FPG that used a flat plate armature and contoured stator. A rectangular block of high explosive (HE) is lit by a row of detonators placed across the width of the HE at a select location along the length of the generator. As the HE burns, the armature takes a characteristic shape determined by the line initiation location. At the appropriate time, the armature first contacts the stator near the input end, then continues to expand into a shape resembling the contoured stator. At late time, the armature contacts the stator at a shallow 1 to 2 degree phasing angle, which rapidly sweeps flux into the load, resulting in a fast current rise time. We have constructed a similar type generator for our present experimental work. It is capable of delivering 20 MA of current with a 2 to 4 μs exponential rise time into suitable loads. This paper describes the design of LLNL's flat-plate FCG, along with results of modeling and simulation performed for its development. Experiments have been carried out using the FPG with seed currents ranging from 0.75 to 1.6 MA using capacitor banks, and up to 2 MA using a helical FCG. Accurate measurements of input and output currents have been made and performance agrees remarkably well with MHD simulations. Challenges faced with calibrating diagnostics and fielding these types of experiments will also be discussed.**

Keywords—magnetic flux compression generator; explosive pulsed power

I. INTRODUCTION

High energy density physics (HEDP) experiments and material science studies are an important part of the wide range of research and development underway at LLNL. To obtain extremely high pressure conditions, explosively driven magnetic flux compression generators (FCGs) are being utilized. LLNL has developed a family of advanced FCGs to be used in our explosively-driven pulsed power experiments. Our high-gain advanced helical generator (AHG) can produce currents of 20 MA and deliver energies of 20 MJ [1]. Our ring-lit coaxial generator (CG), known as the full function test (FFT) device, when coupled with the AHG, can produce currents of 100 MA and deliver energies exceeding 60 MJ [2]. Most recently we have developed a half-scale FFT device known as the Mini-G that is capable of delivering up to 60 MA of current and 8 MJ of energy [3]. Our family of FCGs exhibit fast current rise while delivering high energy to the experimental loads.

Flat plate generators (FPGs) are useful in many flux compression applications. They are well suited for doing material studies in planar geometries, and they enable the use of certain diagnostic techniques, most notably flash X-ray radiography, which would be difficult if not impossible to utilize in coaxial geometries. Typical flat-plate generators have rather slow-rising output currents. This can cause loads to deform significantly before the highest rate of current gain from the generator can be reached. Shearer et al. at LLNL overcame this handicap by developing a version of FPG that used a flat plate armature and contoured stator [4, 5]. We have constructed a similar type generator for our present experimental work. It is capable of delivering 20 MA of current with a 2 to 4 μs exponential rise time into suitable loads. We are using this FPG to perform high energy density physics experiments and material science studies.

II. FLAT-PLATE FCG DESCRIPTION

A. *Flat Plate FCG components and operation*

Figure 1 shows an illustration of LLNL's flat-plate FCG. This is a cutaway view showing only a portion of the width of the components above the stator. The copper armature is 4.65-mm thick, 41-cm wide, and 81cm in length. Between the armature and the HE is a 9.5-mm thick sheet of lexan. The HE is a block of pressed and machined LX-14 that is 6-cm thick, 25-cm wide and 71 cm in length. A steel tamper, 1.25-cm thick, is placed above the HE, and a row of eight RP-1(RL) detonators are installed through the steel tamper and spaced evenly across the width of the HE. The placement of the detonators along the length of the HE is predetermined based on modeling. After the HE is initiated, the burn front propagates in both directions along the length of the HE. The armature first begins to deform just below where the line initiation occurs, then as the burn front propagates, the armature continues to expand, taking on a characteristic shape resembling the contoured stator. At the appropriate time, when seed current has nearly peaked, the armature first contacts the stator near the input end (crowbar). The armature continues to expand until, at late time, the armature is contacting the stator at a shallow 1 to 2 degree phasing angle, which rapidly sweeps flux into the load, resulting in a fast current rise time. Fig. 1 also shows cross section drawings of the armature shape around time of crowbar, and later when the armature shape nearly matches that of the contoured stator.

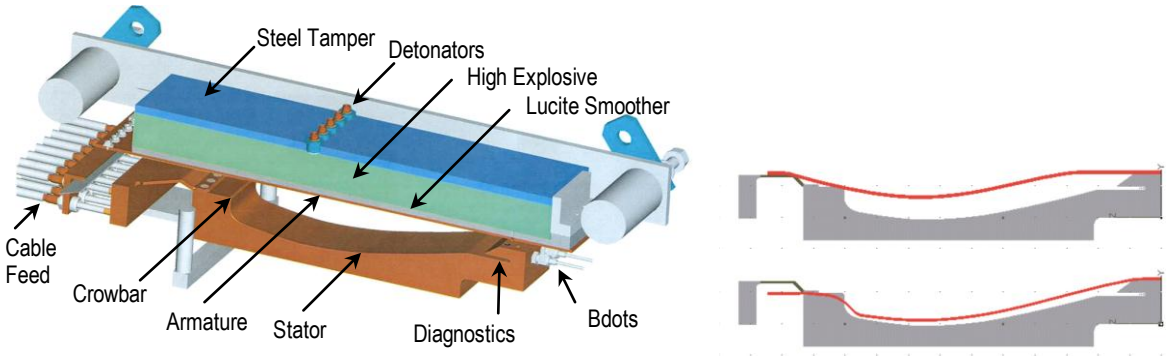

Figure 1. (left) Illustration of LLNL's flat-plate FCG with major components labeled. (right) Cross sections from hydrodynamic modeling showing armature shape around time of crowbar, and later when shape closely matches that of contoured stator.

B. *Input feed cables and insulation*

The seed current for the FCG is supplied through multiple parallel coaxial cables. The cable feedthrough and connections were designed to withstand both high voltage and high current. Our initial design incorporated YK-198 coaxial cable, with a pin and socket connector for easy assembly. This is what is depicted in Fig. 2. In later designs we switched to DS-2310 coaxial cable with a modified swage-lock fitting to clamp around tubing soldered to the center conductor. The DS-2310 cable is nominally 18 Ω and rated for 20 kV DC. The nominal parameters of the cable are 108 nH and 6 mΩ per meter. We hi-pot test each cable before use to 40 kV DC. We have also tested representative cables and connectors using a capacitor bank to demonstrate high current performance up to 175 kA per cable.

C. *Input insulation*

The armature and stator are separated at the input end by an insulation packet. Typically we use multiple layers of Mylar having a total thickness of 1 mm. The corners and edges of the bus bar are radiused to reduce field enhancements. Fig. 3 shows the initial design and results of electrostatic modeling done to evaluate performance. The most worrisome aspect of this implementation is the possibility of surface tracking and flashover across the insulator. To gain confidence we built prototype parts and hi-pot tested the assembly.

D. *Diagnostics*

We incorporated diagnostics into the FPG to monitor input and output current. At the input end we have two Rogowski coil sensors surrounding the center conductors of the coaxial cables. At the output end we have a channel built into the stator for B-dot sensors and Faraday rotation (FR) fiber sensors. The implementation of these diagnostics is similar to what has been reported previously [6].

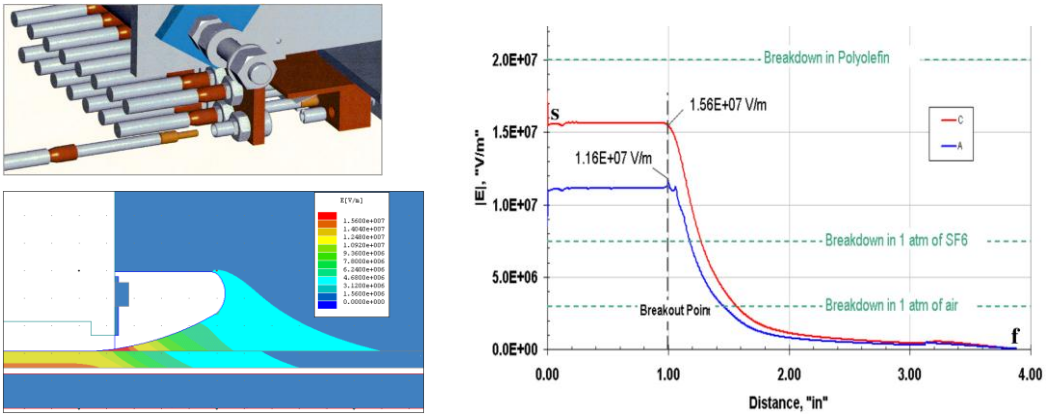

Figure 2. (upper left) Drawing of coaxial cable feedthrough assembly. (lower left) Electrostatic modeling of feedthru component used to reduce field enhancments at triple junction of metal wall, cable insulation, and dielectric gas. (right) Plot of electric field verses distance along cable insulation passing through feedthru. Also shown are typical values for electrical breakdown of insulation and gas materials.

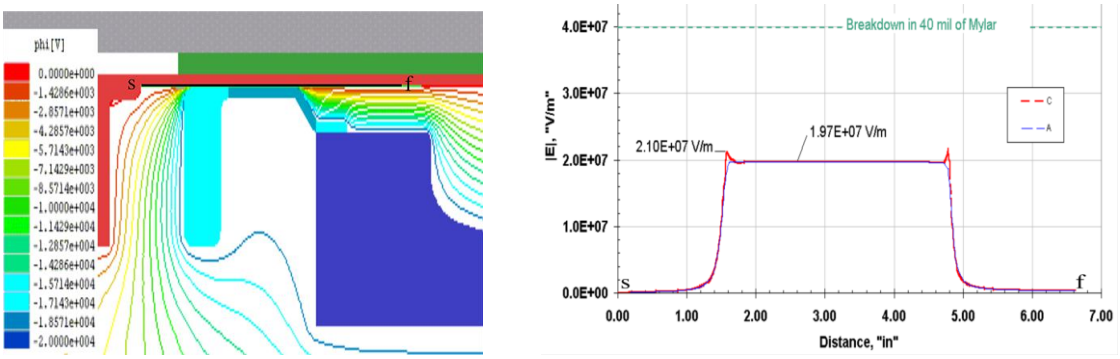

Figure 3. (left) Electrostatic modeling of input insulator region showing equipotential lines for 20 kV applied. (right) Plot of magnitude of electric field verses distance along path length from point s to f showing minimal field enhancements by radiusing edges of busbar. The nominal E-field is 20 kV/mm for 1-mm thick insulation, and the electrical strength of Mylar exceeds 40 kV/mm.

III. Initial Experimental Results

LLNL's first FPG experiment was carried out at an AFRL test site in Albuquerque, NM. This site had the requisite timing, firing, and data acquisition systems, along with a transportable capacitor bank of sufficient size to seed the FPG from a fairly long but safe distance away. The purpose of the first test was to obtain high speed imaging of hydrodynamics along with current gain measurements to compare with MHD modeling predictions. Fig. 4 shows the experimental setup for this first test. The photo on the left shows the side viewed by the high speed camera. The photo on the right shows the opposite side with an argon candle for back lighting. The white structure in both photos is the painted wood support stand. The metal parts above that are the aluminum side panels next to the HE.

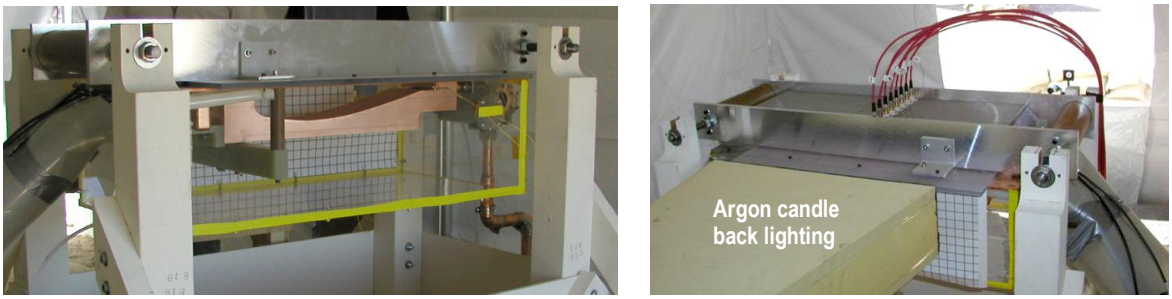

Figure 4. (left).Photo of LLNL's flat-plat FCG set up for first test. (right) Photo of other side with foam box containing argon that is explosively shocked for back illumination while imaging using high-speed rotary mirror camera.

The seed current on this first test was approximately 760 kA. This was measured using Rogowski coils around the input coaxial cable feeds. The Rogowski coils fed electro-optic converters to provide electrical isolation between the experiment and the data acquisition system. The output current was measured with both B-dot sensors and FR fiber sensors located in a stator diagnostic slot. Initially we thought the output current was about 20 MA, but later we determined the current was closer to 18 MA. This uncertainty resulted in part because the FR sensor stopped reporting midway through the exponential current rise, but also because we had more to do to accurately unfold the B-dot data. This will be discussed further in the next section. The high-speed framing camera provided valuable results that confirmed proper operation and verified CALE 2D hydro calculations. Fig. 5 shows those results along with modeling predictions for comparison.

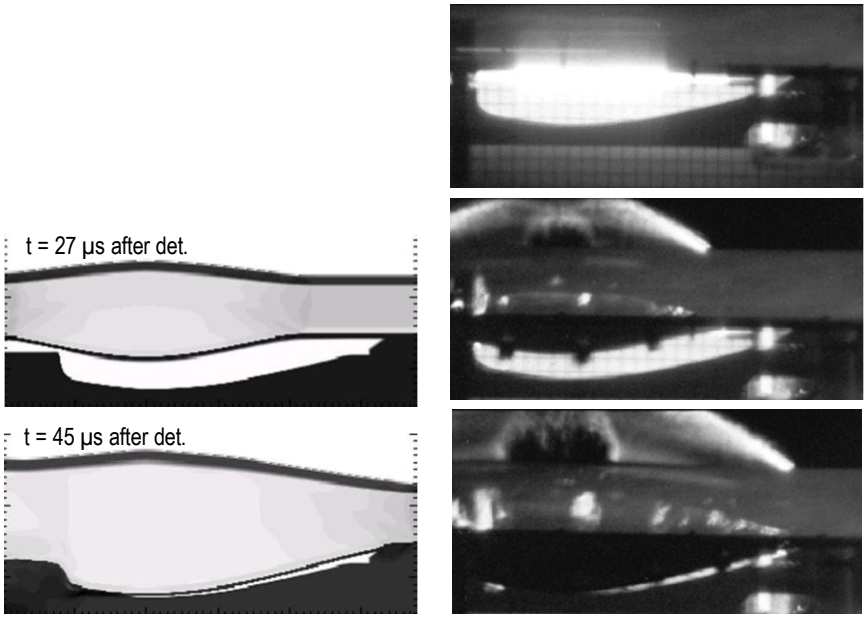

Figure 5. (left).Modeling predictions of armature shape around time of crowbar, and later when armature sweeps along stator at narrow angle. (right) High speed framing camera images before armaturs begins to move and then at times corresponding to modeling predictions.

IV. Interpretation of B-dot Data

One of the challenges in performing experiments using flat plate generators is the 3D nature of the devices, and how to account for changes in geometry during operation that complicate interpretation of diagnostic data. Figs. 6-8 show the various issues and magnitude of errors or uncertainty that can be introduced if one does not take into account these matters. Fig. 9 shows the time varying scale factors derived from 3D modeling that are used to correct the B-dot data.

A. Sensor Location and Edge Effects

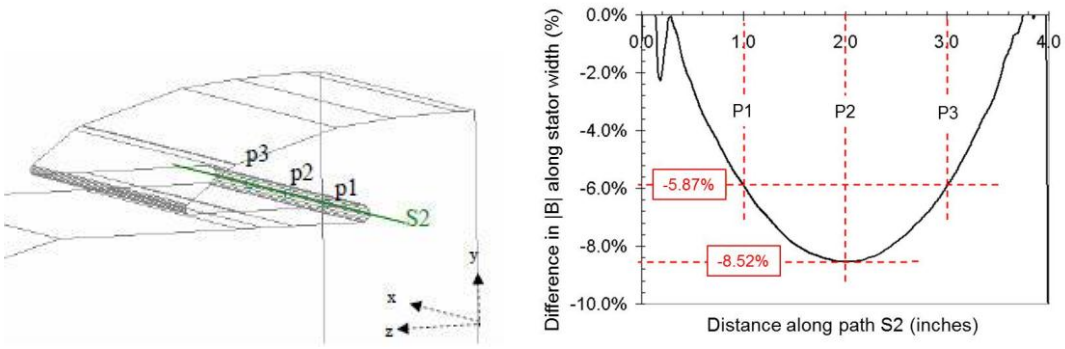

Figure 6. (left).Line drawing from 3D modeling depicting stator shape around diagnostic slot, and position of three B-dot probes spaced an inch apart. (right) Plot of difference in magnitude of magnetic flux density |B| along a path across the width of the stator through three B-dot probes.

B. *Armature-Stator Geometry Dynamics*

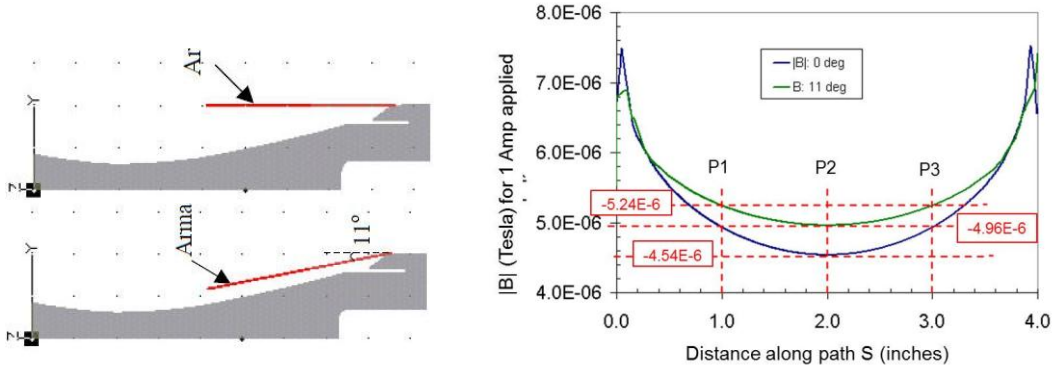

Figure 7. (left) Cross section of stator and position of armature at start of operation and later when armature approaches stator. (right). Plot of magnitude of magnetic flux density along a path across the width of the stator for both cases shown at left for one Ampere of current.

C. *Edge Effects*

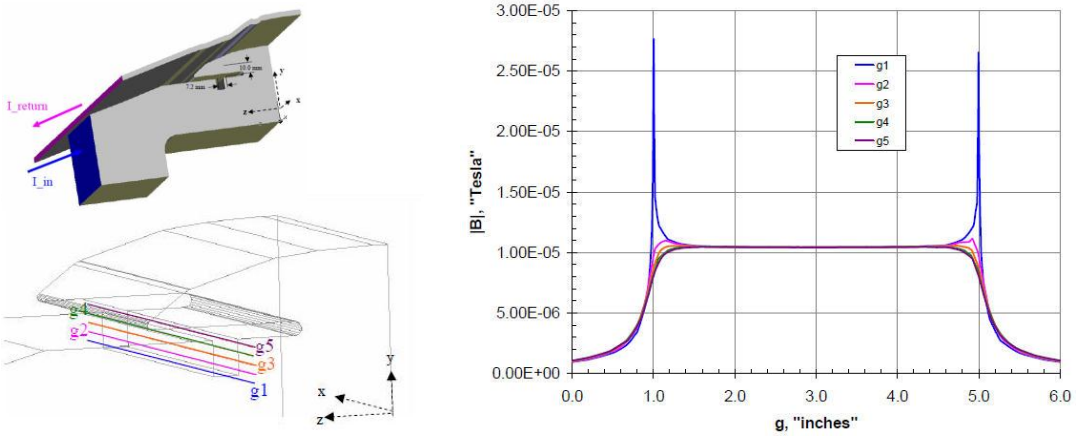

Figure 8. (left) Model of output region showing power flow channel and lines where flux density is compared. (right. Plot of magnitude of magnetic flux density along paths g1-g5 across middle of power flow channel for one Ampere of applied current.

D. *Dynamic Scaling Factors*

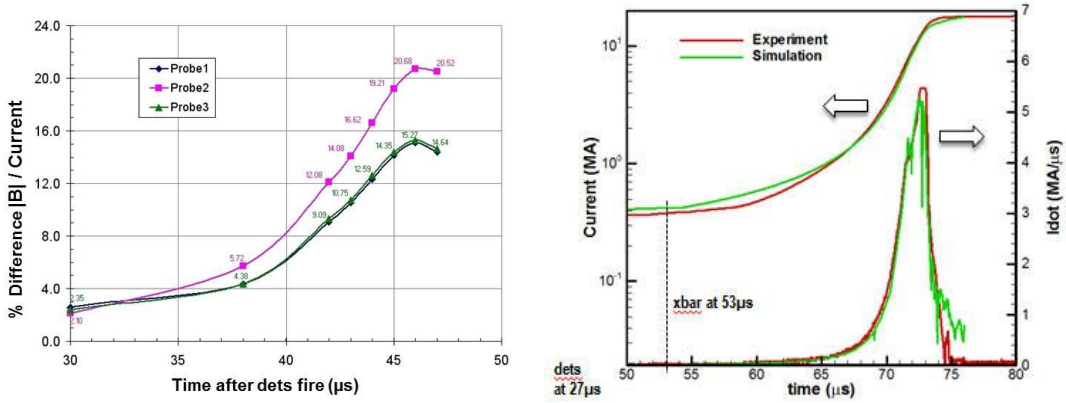

Figure 9. (left) Scale factors derived from 3D modeling, used to correct B-dot data from FPG experiment. (right) Comparison of current waveforms from modeling and experiment data after B-dot correction factors are applied. Peak current from FPG-1 test was 18 MA.

V. ONGOING DEVELOPMENT WORK

Following our first test of the new flat-plate FCG we conducted four more experiments using the system with seed current provided by a capacitor bank. These experiments were carried out at LANL's Ancho Canyon test site. In those experiments the FPG was seeded with 1.6 MA of current. Since then we have upgraded the system to produce greater output currents by incorporating a helical FCG to provide higher seed current. Fig. 10 shows a photo of the two-stage FCG system along with close up views of the cable attachment between the helical and flat-plate FCGs. Further information about our newest experimental capability is provided in the paper by White et al. in these proceedings [7].

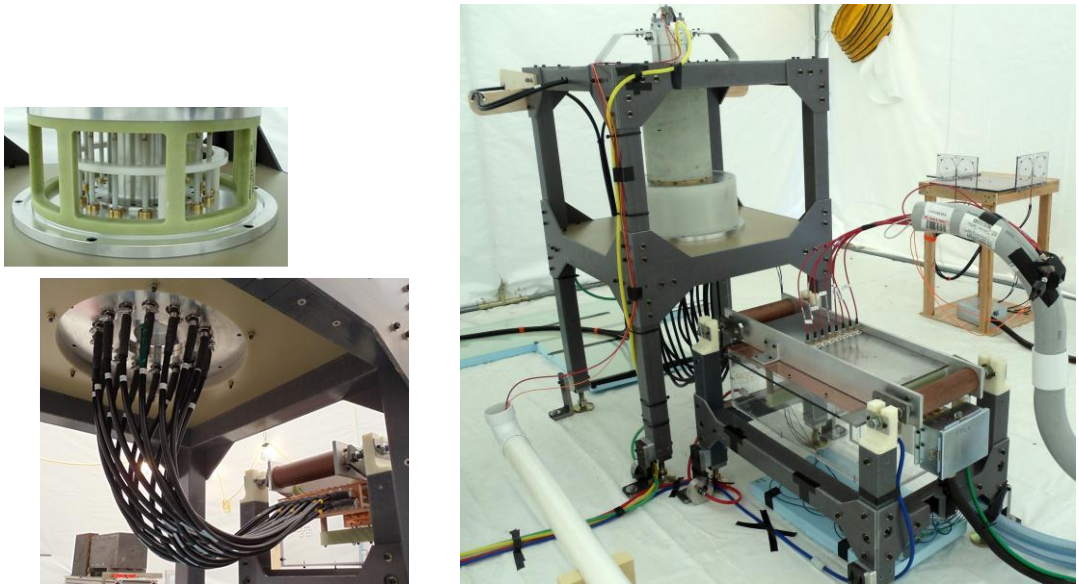

Figure 10. (left) Photos of cable attachement from the helical FCG to the flat-plate FCG. (right) Photo of two-stage FCG system now being used for high energy density physics experiments and material science studies.

ACKNOWLEDGMENTS

The authors acknowledge and appreciate the collaboration of AFRL in executing LLNL's first FPG experiment, especially the assistance of Jim Degnan, Jerry Kiuttu, Jerry Parker, Mark Lehr, Sean Coffey and their capable technical staff. The authors also acknowledge and appreciate the collaboration of LANL in executing four additional FPG experiments at their Ancho Canyon test site, especially the assistance of Jim Goforth, Hank Oona, Lenard Tabaka and Dennis Herrera. This work performed under the auspices of the U.S. Department of Energy by Lawrence Livermore National Laboratory under Contract DE-AC52-07NA27344.

REFERENCES

[1] D. B. Reisman, *et al.*, "The advanced helical generator", *Rev. Sci. Instr.*, ***81*** *(*2010), p. 034701.

[2] D. B. Reisman, *et al.*, "Note: The full function test explosive generator", *Rev. Sci. Instr.*, ***81*** *(*2010), p. 036109

[3] D. B. Reisman, *et al.*, "Explosive Flux Compression Generators at LLNL," these proceedings.

[4] J. W. Shearer *et al.*, "Explosive-driven magnetic-field compression generators," J. Appl. Phys. **39**, 2102 (1968).

[5] D. J. Steinberg and J. W. Shearer, "Flat-plate experiments on magnetically accelerated metal liners," Proc. Megagauss IIII Conference, Santa Fe, NM, 1986

[6] D. A. Goerz, *et al.,* "Implementation of pulsed power diagnostics on explosive flux compression generators at LLNL," The 13th International Conference on Megagauss Magnetic Field Generation and Related Topics, Suzhou, China, 2010.

[7] A. D. White, *et al*, "Explosive pulsed power experimental capability at LLNL," these proceedings.